American Mineralogist, Volume 61, pages 944–955, 1976

The stability relations of the wolframite series

L. C. Hsu

Nevada Bureau of Mines and Geology, and Department of Geology and Geography
Mackay School of Mines, University of Nevada, Reno, Nevada 89507

Abstract

The stability relations of the two end members of the wolframite series are experimentally determined by conventional hydrothermal and solid-buffer techniques. At P_f = 1000 bars, ferberite ($FeWO_4$) coexists stably with hematite over a temperature range of 400° to 900°C, but begins to decompose according to the reaction $2FeWO_4 + \frac{1}{2} O_2 = Fe_2WO_6 + WO_3$ above about 540°C and at f_{O_2} values defined by the Cu_2O–CuO buffer. Fe_2WO_6, not reported in nature, has a = 4.592Å, b = 16.800Å, c = 4.972Å and belongs to *Pmmn* with Z = 4. Huebnerite ($MnWO_4$) is stable at all temperatures and all f_{O_2} values attainable by the solid buffer technique.

Addition of sulfur to the system results in the reactions: $FeWO_4 + 3/2\ S_2$ (or $2S_2$) = FeS (or FeS_2) + $WS_2 + 2O_2$ and $MnWO_4 + 3/2\ S_2 = MnS + WS_2 + 2O_2$. At 1000 bars and 577°C the reaction for ferberite to form FeS and WS_2 passes through the following points on the log f_{O_2}–log f_{S_2} diagram: (−19.4, −3.0), (−21.8, −7.1), and (−24.9, −12.7). The reaction curve for huebnerite does not differ much from that for ferberite in slope and position.

The compositional variation of the wolframite series in terms of Mn/Fe cannot be used to evaluate such physico-chemical variables during ore formation as f_{O_2}, pressure, and in particular temperature.

Introduction

Minerals of the wolframite group form a complete solid solution series between the two end-members, ferberite, $FeWO_4$, and huebnerite, $MnWO_4$. Wolframite is a mineral characteristic of relatively high-temperature hydrothermal veins and hydrothermally or pneumatolytically altered granitic rocks (greisen) associated with cassiterite, arsenopyrite, molybdenite, tourmaline, topaz, fluorite, and other minerals. The wolframite-group minerals are also found in moderate and low-temperature veins as well as in contact metamorphic deposits adjacent to granitic intrusions.

The concept that manganese/iron ratios of members of the wolframite group may vary according to the conditions of formation was recently called to attention by Taylor and Hosking (1970). Some workers have considered that a low Mn/Fe ratio in wolframite corresponds to a low temperature of formation (*e.g.* Baumann and Starke, 1964, 1965; Bolduan, 1954; Lawrence, 1961). However, results from the U.S.S.R. indicate exactly the reverse (*e.g.* Churikov, 1959; Ganeev and Sechina, 1960). Chemical analyses of wolframite by Barabanov (1961) show that its composition varies considerably not only in a given deposit but in a single vein. He concluded that (1) wolframite is a product of local reactions and is not introduced into the vein as such; and (2) the composition of wolframite is determined not by the depth and temperature of its formation, nor by the composition of the juvenile solutions, but by the composition of surrounding rocks.

The contradictory conclusions regarding the composition of wolframite as a temperature indicator prompted an experimental investigation under hydrothermal conditions to determine the stability relations of wolframite as a function of physico-chemical parameters such as temperature, pressure, and oxygen and sulfur fugacities. Because it has been demonstrated for many silicate minerals that the stability of the Fe^{2+} end-member is much more sensitive to the variation of f_{O_2} than is the Mn^{2+} end-member (*e.g.* Hsu, 1968, on almandine and spessartine), it seems possible that the composition of wolframite might be strongly affected by the oxidation state of the environment. The common association of wolframite with some sulfide minerals indicates that sulfur is commonly present and may play a role in the stability of wolframite.

Experimental methods

Conventional hydrothermal equipment and techniques were employed in this study. All the experiments were made in cold-seal pressure vessels (Tuttle, 1949) fabricated from René 41 or SS316 alloy. Hydrostatic pressure was generated by an air-driven SC hydraulic pump and was monitored continuously by Astragauges which were calibrated against a 12-inch factory-calibrated Heise gauge and are believed to be accurate to ± 2 percent of the stated value. Pressure vessels were heated in horizontal, split-wound Lindberg Hevi-Duty furnaces. Furnace temperatures were controlled by solid-state Series 676, Temperature Controllers to within ± 2°C and individual runs were maintained with temperature fluctuation always within ± 5°C. The temperatures in each pressure vessel were calibrated according to the method described by Boettcher and Kerrick (1971) using the same closure nut and the thermocouple assemblies loaned from Boettcher.

Because one of the chief aims of the study was to determine the effect of oxidation state on the stability of wolframite, f_{O_2} was controlled in all runs by using the buffer technique devised by Eugster (1957). Huebner (1971) gave a thorough review and description of this technique and listed the equations for all presently available buffer curves with pressure corrections.

For simultaneous control of f_{O_2} and f_{S_2}, a solid-buffer technique modified after that of Eugster and Skippen (1967) and Huebner (1971) was adopted. The method of controlling f_{O_2} and f_{S_2} through proper choice of pH and ΣS as described by Barnes (1971) could not be used because the limited size of the charge capsule could not accommodate sufficient quantity of aqueous solution. The available solid oxide and sulfide pairs used in controlling f_{O_2} and f_{S_2} simultaneously are shown in Figure 1. These equilibria have been calculated and plotted at 577°C and 1000 bars based on available thermodynamic data, chiefly those compiled by Robie and Waldbaum (1968). The solid circles in the figure represent invariant points at given pressure and temperature. In order to buffer the runs under these conditions, the charge with excess H_2O (about 5 mg) was enclosed in a crimped gold capsule of 0.100″ O.D., then solid buffer assemblages consisting of both oxide and sulfide (*e.g.* magnetite + pyrite + hematite) with excess H_2O (about 35 mg) were enclosed together with the crimped capsule in a sealed gold capsule of 0.200″ O.D. The crimped inner capsule allowed the free passage of the gas species between the two capsules. For runs buffered at the crosses in the figure, which are intersections of f_{O_2} and f_{S_2} curves at the given pressure and temperature, the charge with excess H_2O was enclosed in a crimped gold capsule of 0.100″ O.D. A solid sulfide pair with excess H_2O (about 15 mg) was then enclosed together with the crimped capsule in a sealed platinum capsule of 0.165″ O.D. Finally, a solid oxide pair with excess H_2O (about 30 mg) was enclosed together with the platinum capsule in a sealed silver capsule of 0.220″ O.D. The sealed platinum capsule allowed free passage of only hydrogen gas molecules, through which f_{O_2} was controlled. The sulfur gas molecules were confined within the platinum capsule, though free passage to the crimped gold capsule was permitted. When the sulfide pair buffers a relatively high f_{S_2}, the inner wall of the platinum may yield a thin film of black PtS. To what extent this thin film of PtS affected the hydrogen diffusion is not clear. However, periodical change of the platinum capsule probably assured the free diffusion of hydrogen. The two buffer assemblages can be expressed as O_BS_B, HOS [X, HOS] and O_B, OH(S_B, HOS [X HOS]), respectively, according to the nota-

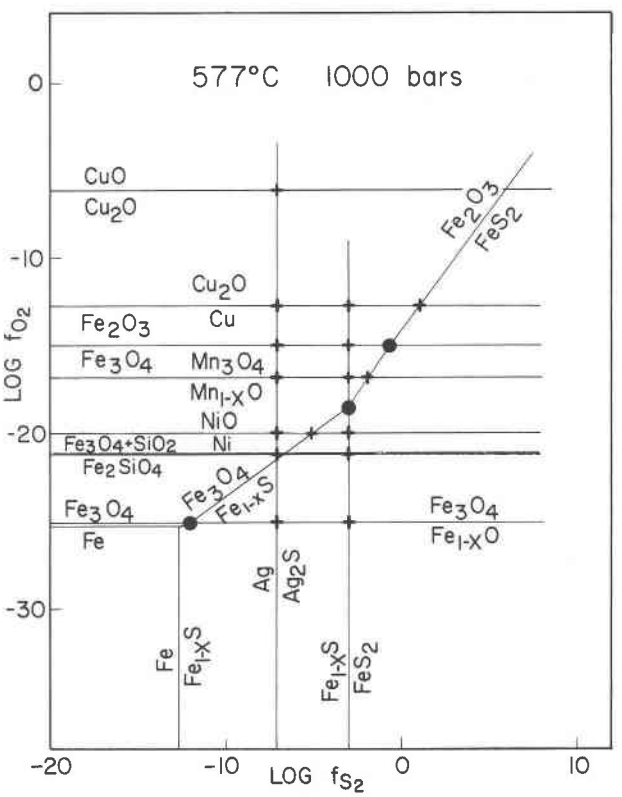

FIG. 1. Log f_{O_2}–log f_{S_2} plot showing the position where both f_{O_2} and f_{S_2} can be controlled simultaneously. See text for explanation of circles and crosses.

tions of Eugster and Skippen (1967). Abbreviations for solid buffer assemblages are listed in Table 1 along with those of synthetic phases.

Two end members, ferberite and huebnerite, as well as nine intermediate compositions of the wolframite group at 10 mole percent intervals were synthesized hydrothermally from Baker Analyzed reagent grade tungstic acid and iron powder and Atomergic Chemicals Company electrolytic manganese powders. All sulfide phases relevant to the experiments were synthesized hydrothermally from Gollard-Schlesinger Chemicals Corporation crystal lump sulfur and Baker Analyzed metal powders. Mixtures of synthetic wolframite and its synthetic decomposition counterparts in wolframite stoichiometry were used as starting material in each run for bracketing experiments.

All runs were brought to temperature at pressure in an hour and were quenched to room temperature with a jet of compressed air in 10 minutes at nearly constant pressure. Condensed run products were examined with a petrographic microscope and Norelco X-ray diffractometer equipped with a graphite-monochromator using Cu$K\alpha$ radiation and a scintillation counter.

For determination of unit-cell parameters, Si powder (a=5.43012Å) or NaCl powder (a=5.63937Å) was used as an internal standard. At least one oscillation at ¼° 2θ per minute scan speed and ½″ per minute chart speed was made for each determination when more than six peaks were used; three oscillations at the same speed were made where fewer than three peaks were used. Measurements were made to 0.002° 2θ, and results averaged. Unit cell parameters were calculated on the CDC 6400 computer at the University of Nevada System Computing Center. The computer program employed for least-squares refinement of crystallographic lattice constants was written by Appleman and Evans (1973).

Experimental results

Phase characterization

Wolframite. Eleven compositions of the wolframite group at 10 mole percent intervals were synthesized hydrothermally at 650°C and 1000 bars fluid pressure. The ferberite end-member formed black, opaque crystals in short prisms of average dimension 15 × 20μm. The ends of the prisms usually were tapered by pinacoids. Reddish-brown color was observed only in thin flakes and with convergent light. In contrast, the huebnerite end-member was yellowish to reddish brown in color with varying pleochroism. It crystallized in prisms of smaller size, 5 × 10μm on average. A small extinction angle $Z\Lambda c$ = 17° was also observed. No systematic variation in

TABLE 1. Abbreviations and compositions of synthetic phases and oxygen, sulfur, and oxygen-sulfur buffer assemblages

Ad = Alabandite, MnS	MH = Magnetite-Hematite
Fb = Ferberite, $FeWO_4$	CCU = Copper-Cuprite
Ft = Fe_2WO_6	NNO = Nickel-Nickel Oxide
Hb = Huebnerite, $MnWO_4$	FMQ = Fayalite-Magnetite + Quartz
Hm = Hematite, Fe_2O_3	WM = Wüstite-Magnetite
Mt = Magnetite, Fe_3O_4	IW = Iron-Wüstite
Pg = Partridgeite, Mn_2O_3	IQF = Iron + Quartz - Fayalite
Po = Pyrrhotite, $Fe_{1-x}S$	PR = Pyrite-Pyrrhotite
Py = Pyrite, FeS_2	SA = Silver-Argentite
Tn = Tungstenite, WS_2	MPH = Magnetite-Pyrite-Hematite
To = WO_3	MPR = Magnetite-Pyrite-Pyrrhotite
HP = Hausmannite-Partridgeite	WMR = Wüstite-Magnetite-Pyrrhotite
CT = Cuprite-Tenorite	IWR = Iron-Wüstite-Pyrrhotite

unit-cell parameters was found in both ferberite and huebnerite synthesized at different temperatures and different oxygen fugacities, although Schröcke (1969) described a slight deviation from the stoichiometric composition for ferberite at 1000°C as a result of variation in P_{O_2}. The cell parameters for ferberite and huebnerite are, respectively, in Å a=4.733(2) and 4.829(1), b=5.709(2) and 5.759(1), c=4.964(3) and 4.9971(1), and β=90° and 91°10′(3)′.

The nine intermediate members showed optical and crystallographic properties intermediate between the two end-members. The variation of the unit-cell parameters with chemical composition in wolframite has been investigated in detail by several authors (*e.g.* Sasaki, 1959; Berman and Campbell, 1957; Baumann and Starke, 1964; and Sleight, 1972). A fast, yet reliable, method of determining the wolframite compositions was developed from the synthesized materials using quartz as an internal standard. Figure 2 shows the variation of the d_{200} of the synthetic wolframites as a function of the composition (*i.e.* Mn/Fe ratio). The $\Delta 2\theta$'s between 102 of quartz and 200 of wolframite increase linearly with increasing mole percent of $MnWO_4$. The sensitivity and accuracy of this figure could be improved by use of Fe$K\alpha$ radiation, because of its better angular resolution.

Fe_2WO_6. Ferric tungstate occurred as an oxidation product of ferberite. It was black and opaque to semi-translucent in thin flakes. The crystals usually appeared as short prisms in rectangular shape instead of tapering off at the ends. From the barely visible reddish-brown interference color, parallel extinction was recognized. According to some workers (*e.g.* Bayer, 1962) similarities in unit cell parameters suggest that Fe_2WO_6 has the columbite–tantalite structure (space group *Pcan*). However, Bayer failed to index many reflections present in Fe_2WO_6. Through an analysis of the systematic extinctions of diffraction rings, Trunov and Kovba (1966) assigned either *Pmmn* or *Pnma* as the space group for Fe_2WO_6. A careful indexing with the aid of a computer program in the present study indicated that the appropriate space group is *Pmmn* with Z=4. The powder diffractogram for Fe_2WO_6 synthesized at 840°C, 1000 bars, and f_{O_2} controlled by the HP buffer (FT25) is consistent with that for Fe_2WO_6 synthesized at 1000°C and 1 atm by Trunov and Kovba (1966). The cell parameters obtained for Fe_2WO_6 are: a=4.592(1), b=16.800(2), c=4.972(1)Å.

WO_3. Tungsten trioxide, together with Fe_2WO_6, occurred as an oxidation product of ferberite. It formed as minute greenish-yellow grains less than 2μm in diameter and had a very high birefringence with mean refractive index higher than 1.90. The indices of refraction α, β, and γ could not be determined accurately because of their high values and the minute size of the crystals. Although WO_3 has been reported to exist in many different polymorphs (*e.g.* Ueda and Ichinokawa, 1951; Tanisaki, 1960a, b), none of the various high-and low-temperature polymorphs has been reported to be quenchable to room temperature. However, many of these reported phases have been found at room temperature when incorporated with 2 or 3 mole percent Nb_2O_5 (Roth and Waring, 1966). The room-temperature form of WO_3 belongs to the monoclinic system; its X-ray powder diffraction data are consistent with those listed in Roth and Waring (1966, Table 14). The cell parameters obtained for WO_3 at room temperature are: a=7.302(1), b=7.537(1), c=3.846(1)Å, β=90°52′(1)′.

Sulfides. With the introduction of sulfur into the system, tungstenite, WS_2, was the major sulfide mineral; the others are pyrite, pyrrhotite, and alabandite. Tungstenite occurred as minute, opaque flakes that are optically indistinguishable from molybdenite. The X-ray data indicate that the hydrothermally synthesized tungstenite belongs to the 2*H* polytype with the cell parameters a=3.156(1), c=12.356(2)Å. The other sulfides always yielded weak X-ray diffraction peaks because of their strong absorption of the Cu$K\alpha$ radiation. Their presence was in most cases indicated by their strongest peaks (*e.g., 200* at 34.3° 2θ for alabandite, *200* at 33.1° 2θ for pyrite, and *102* at 43.8° 2θ for pyrrhotite). The pyrrhotite was hexagonal as indicated by a single, sharp, symmetrical

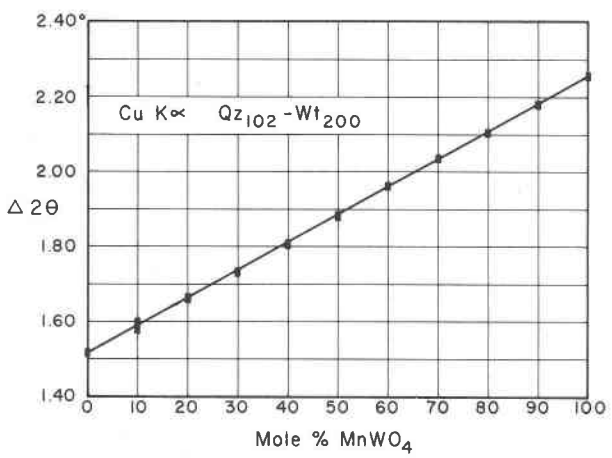

FIG. 2. Variation of d_{200} of wolframite as a function of its composition.

TABLE 2. Experimental results of wolframite stability as a function of f_{O_2} and T at P_f = 1000 bars

Run No**	Starting Mix	Temperature (°C)	Buffer	Duration (Hours)	Condensed Run Products***
FB 95	Fb+Ft+To	900	HP	80	Ft+To+(Fb)
97	Fb+Ft+To	820	HP	178	Ft+To+(Fb)
106	Fb+Ft+To	763	HP	548	Ft+To+(Fb)
139	Fb+Ft+To	700	HP	136	Ft+To+(Fb)
129	Fb+Ft+To	500	HP	1692	Ft+To+(Fb)
86	Fb+Ft+To	400	HP	2162	Ft+To+(Fb)
104	Fb+Ft+To	898	CT	64	Ft+To+(Fb)
54	Mt+To	797	CT	96	Ft+To+(Fb+Mt)
55	Hm+To	797	CT	96	Ft+To+(Hm)
59	Hm+To	750	CT	148	Ft+To+(Hm)
70	Fb+Ft+To	750	CT	171	Ft+To+(Fb)
77	Fb+Ft+To	690	CT	262	Ft+To+(Fb)
75	Fb+Ft+To	576	CT	602	Ft+To+(Fb)
130	Fb+Ft+To	500	CT	2114	Fb+(Ft+To)
168	Ft+To+Fb	500	CT	2156	Fb+(Ft+To)
134	Ft+To+Fb	410	CT	4781	Fb+(Ft+To)
84	Ft+To+Fb	900	MH	46	Fb
60	Hm+To	800	MH	88	Fb
61	Hm+To	750	MH	112	Fb+(To+Hm)
69	Ft+To+Fb	750	MH	170	Fb
30	Ft+To+Fb	702	MH	97	Fb
131	Ft+To+Fb	500	MH	1467	Fb+(Ft+To)
85	Ft+To+Fb	400	MH	2162	Fb
37	Hm+To+Fb	404	MH	998	Fb
38	Hm+To+Fb	309	MH	1865	Fb+(Hm+To)
146	Ft+To+Fb	590	CCU	624	Fb
167	Ft+To+Fb	500	CCU	2156	Fb+(Ft+To)
166	Ft+To+Fb	410	CCU	2392	Fb+(Ft+To)
165	Ft+To+Fb	600	NNO	182	Fb
164	Ft+To+Fb	600	IQF	162	Fb
FT 25	Fb+Hm+Ft	840	HP	160	Ft
23	Fb+Hm+Ft	760	HP	252	Ft+(Fb+Hm)
05	Hm+To	705	HP	71	Ft+(Hm+To)
18	Fb+Hm+Ft	700	HP	348	Ft+(Fb+Hm)
19	Fb+Hm+Ft	600	HP	413	Ft+(Fb+Hm)
20	Fb+Hm+Ft	550	HP	812	Ft+(Fb+Hm)
24	Fb+Hm+Ft	840	CT	165	Ft
22	Fb+Hm+Ft	760	CT	204	Ft+(Fb+Hm)
21	Fb+Hm+Ft	600	CT	413	Ft+(Fb+Hm)
26	Fb+Hm+Ft	500	CT	1479	Ft+(Fb+Hm)
28	Fb+Hm+Ft	590	CCU	624	Fb+Hm
27	Fb+Hm+Ft	500	CCU	1478	Fb+Hm+(Ft)
06	Hm+To	705	MH	264	Fb+Hm+Mt
15	Ft+Hm+Fb	650	MH	192	Fb+Hm+Mt
HB 16	Pt+To+Hb	900	HP	65	Hb
20	Pt+To+Hb	750	HP	112	Hb
14	Pt+To+Hb	600	HP	400	Hb+(Pg+To)
13	Pt+To+Hb	400	HP	1600	Hb+(Pg+To)

*Several runs at P_f=2000 bars show no difference from runs at P_f=1000 bars.
**FB: bulk composition of $FeWO_4$, FT: bulk composition of Fe_2WO_6,
HB: bulk composition of $MnWO_4$.
***Phase or phases within parentheses are interpreted as metastable.

102 reflection (Arnold, 1966). No attempt was made to determine the composition of pyrrhotite.

Effect of f_{O_2} *on wolframite stability*

Because wolframite contains Fe and Mn, elements capable of existing in different valence states, the oxidation state of the environment may affect the stability of the mineral. Results of a series of hydrothermal runs conducted at $P_f = 1000$ bars on the bulk compositions of the two end-members, ferberite and huebnerite, using the solid oxygen-buffer technique, are presented in Table 2.

Huebnerite remains stable throughout the temperature range of 400° to 900°C and the f_{O_2} values defined by the IQF to HP buffers. This is consistent with the result of Schröcke (1969), who found that huebnerite remains stoichiometrically stable at 1000°C for the P_{O_2} range of $10^{-22.5}$ to at least 1 atm.

On the other hand, the stability field of ferberite is somewhat affected by the f_{O_2}, because Fe^{2+} is more susceptible to oxidation than Mn^{2+}, as shown by Hsu (1968) for almandine–spessartine. Still, the effect of f_{O_2} on ferberite stability is not as great as one might expect from other ferrous minerals, as shown by Figure 3. At $P_f = 1000$ bars, ferberite remains intact even at an oxidation state where magnetite is completely oxidized to hematite. Ferberite decomposes only under the conditions of high f_{O_2} defined by the CT and HP buffer assemblages. The oxidation products under such conditions consist of WO_3 and Fe_2WO_6 rather than Fe_2O_3 as one might expect. Berman and Campbell (1957) reported that ferberite decomposes to Fe_2WO_6 and WO_3 when heated in air at 950°C, whereas huebnerite remains intact. They found that wolframite stable in air at 950°C contains approximately 60 mole percent $MnWO_4$. Neither Fe_2WO_6 nor WO_3 has ever been reported to occur in nature, although Kittl (1951) and Kittl and Kittl (1965) reported a "light wolframite" possibly containing Fe_2WO_6; the low density was later proved by Escobar *et al.* (1971) to be due to pores of microscopic size in the crystals. The absence of these two compounds in nature can be interpreted as meaning either (1) that the oxidation state of the environment in which ferberite is formed rarely attains f_{O_2} values as high as those defined by the CT and HP buffers, or (2) that Fe_2WO_6 or WO_3, once formed, quickly becomes hydrated as ferritungstite, $Ca_2Fe_2^{2+}Fe_2^{3+}(WO_4)_7 \cdot 9\ H_2O$, tungstite, $WO_3 \cdot H_2O$, or hydrotungstite, $H_2WO_4 \cdot H_2O$ as the temperature falls, or is incorporated into limonite or psilomelane in an amorphous form. An important fact is that the ferrous compound, ferberite, is unusually resistant to oxidation even at lower temperatures, as inferred from the slope of the boundary curve which is gentler than all the buffer curves.

With only one relatively tight bracket in Figure 3, the slope of the boundary curve for the reaction

$$4\ FeWO_4 + O_2 = 2\ Fe_2WO_6 + 2\ WO_3 \qquad (1)$$

could not be obtained with certainty, although a best-fitting curve could be drawn. The uncertainty of the curve, however, probably does not exceed one-half unit of log f_{O_2} at 900°C. The straight line in Figure 4, a log f_{O_2} *vs.* $1/T$ diagram, represents the data points recalculated from the curve in Figure 3 to a 1 bar standard state, *i.e.* after deduction of the contribution of the $\int_1^P \Delta V_s dP$ term from the Gibbs free energy of reaction. The probable uncertainty in slope is shown as light lines. The molar volume of 40.38 cm³/mole for ferberite and 31.61 cm³/mole for WO_3 from Robie and Waldbaum (1968) and the molar volume of 57.78 cm³/mole for Fe_2WO_6 obtained from this work were used.

The slope of the reaction curve obtained from Figure 4 is 8917±1330 °K. The 15 percent uncertainty of the slope surpasses any experimental errors and is

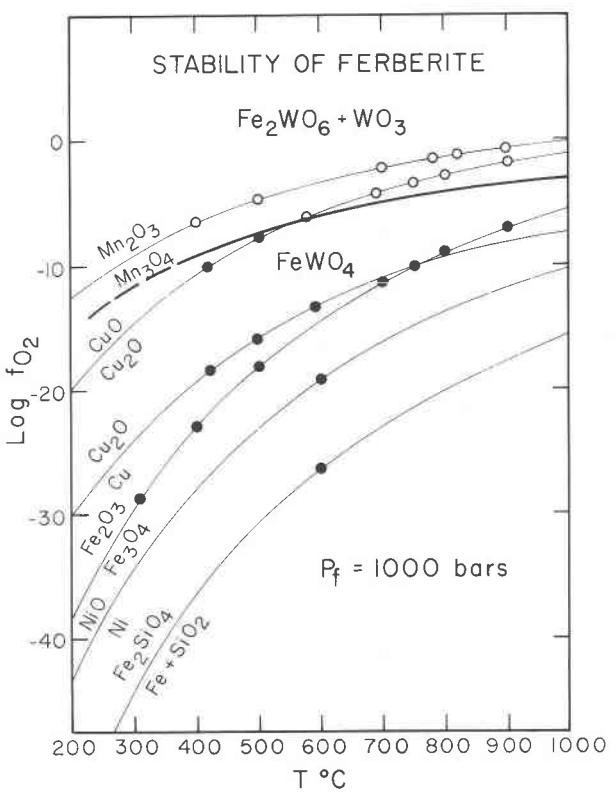

FIG. 3. The stability of ferberite shown on log f_{O_2}–T plot.

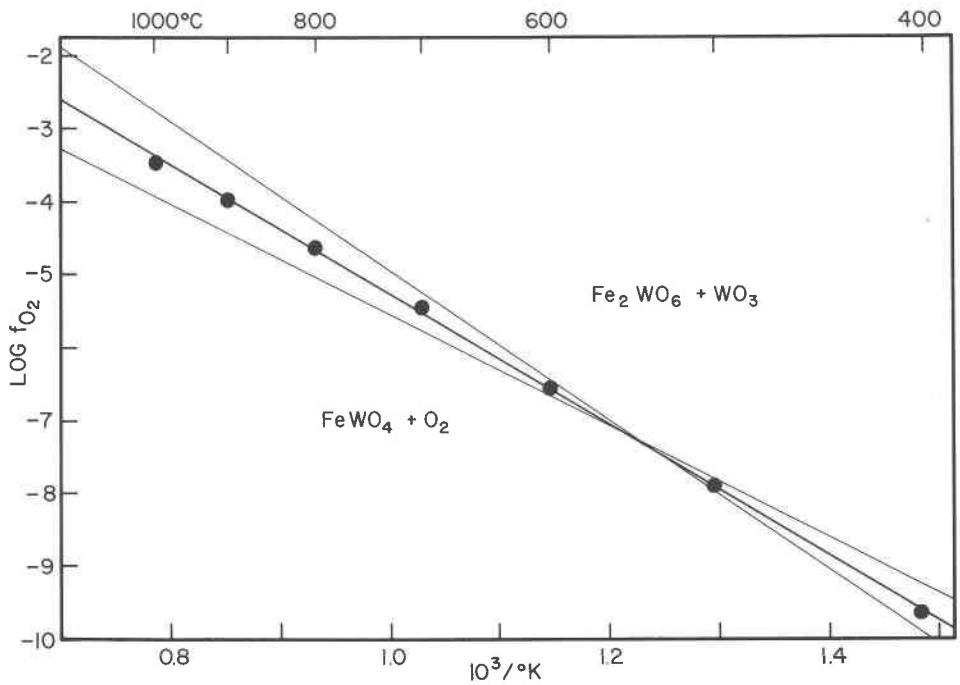

FIG. 4. The log f_{O_2}–$1/T$ plot for the equilibrium curve of the equation (1) at 1 atm. Light lines indicate uncertainty in the slope of the curve.

transferred to the calculations to follow. Simple substitution and calculation yield the equations

$$\log f_{O_2} = 3.64 - \frac{8917}{T} \quad (2)$$

and

$$\log K = 2 \log a_{Fe_2WO_6} + 2 \log a_{WO_3} - 4 \log a_{FeWO_4} - \log f_{O_2} \quad (3)$$

where K is the equilibrium constant of reaction (1) and the a's are the activities of the solid phases assuming stoichiometric composition; these activities are taken as unity at 1 bar standard state. The standard enthalpy of reaction (1) calculated from the slope is −10,201 cal/mole $FeWO_4$. The standard free energy of the reaction is calculated by substituting the expression $\Delta G° = -RT\ln K$ into equations (2) and (3), yielding

$$\Delta G_r° = 16.66T - 40{,}804 \text{ cal} \quad (4)$$

The equilibrium oxygen fugacity for reaction (1) at any P and T can be expressed by including a correction term for the effect of total pressure on the solid phases (Eugster and Wones, 1962) to equation (2)

$$\log f_{O_2} = 3.64 - \frac{8917}{T} + 0.0911 \frac{P-1}{T} \quad (5)$$

Equation (5) appears to be very similar in order of magnitude to that for the Mn_3O_4–Mn_2O_3 buffer determined by Huebner and Sato (1970).

The lower f_{O_2} limit for the stability of $FeWO_4$ was not determinable in the hydrothermal system. Schröcke and Trumm (1968) developed a method to measure the oxygen partial pressures of crystalline phases containing oxides by means of indicators. The samples and indicators were contained in evacuated ampules made of quartz glass, and the ends of the ampules could be held at different temperatures. By using small pieces of metals as indicators, they determined the low P_{O_2} limit of $FeWO_4$ to be $10^{-21.5}$ atm at 1000°C, which is about one order of magnitude higher than that of $MnWO_4$.

The direct oxidation of ferberite to Fe_2O_3 and WO_3 may take place at much higher temperatures than were used in this study, as is suggested by a Schreinmaker's analysis of the f_{O_2}–T relations of the relevant phases (Fig. 5). Bayer (1962) reported the decomposition of Fe_2WO_6 to Fe_2O_3 + WO_3 at 1100°C under atmospheric conditions. The coexistence of ferberite with hematite inferred in Figure 5 is also confirmed experimentally in this study on a bulk composition equivalent to Fe_2WO_6 (Table 2).

Effect of f_{O_2} *and* f_{S_2} *on wolframite stability*

The introduction of sulfur into the hydrothermal system of ferberite bulk composition results in the

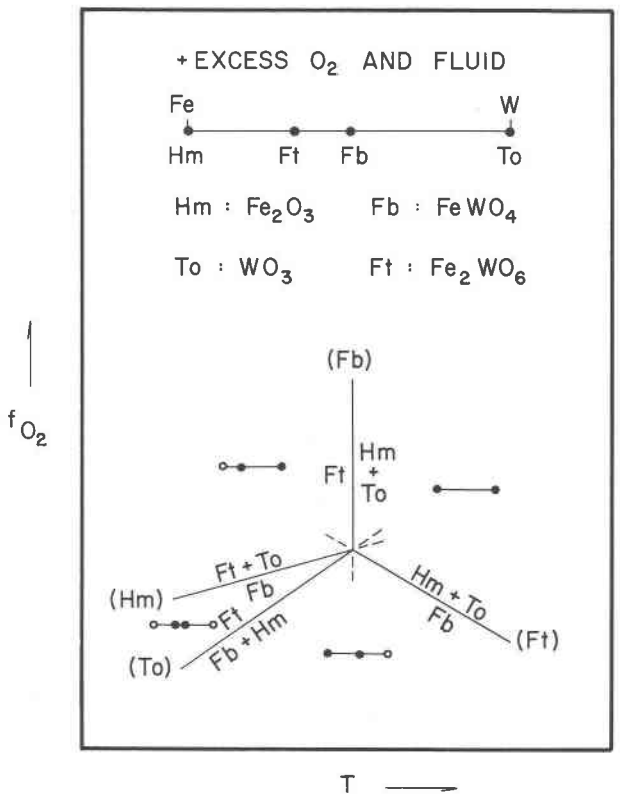

FIG. 5. The f_{O_2}–T relations of the phases in the system Fe-W-O.

formation of tungstenite (WS_2) and pyrrhotite ($Fe_{1-x}S$) and/or pyrite (FeS_2), depending on the f_{S_2} values which were controlled along with f_{O_2} values by various solid buffer assemblages. The reaction for the decomposition of ferberite involving sulfur and oxygen can be written as

$$FeWO_4 + 3/2\ S_2\ (\text{or } 2S_2) = WS_2 + FeS\ (\text{or } FeS_2) + 2\ O_2 \quad (6)$$

As shown in Table 3, few runs actually went to completion even if the duration exceeded a month. This phenomenon may be attributed to either (1) an extremely slow reaction rate when sulfur is involved, as is shown by the preliminary investigation of the system almandine–sulfur–water at 700°C and 1 kbar (MacRae and Kullerud, 1972), or (2) a very weak buffering power exerted by the sulfide buffer assemblages, *i.e.* the buffer sulfide does not react or release sulfur as readily as does the buffer oxide. Nevertheless, the extent of reaction was sufficient to yield an unambiguous indication as to the direction of reaction. This, in conjunction with the consistency of the experimental results, provides the basis for delineating the equilibrium curve shown in Figure 6, a log f_{O_2}–log f_{S_2} plot of the stability of ferberite at 577°C and 1000 bars fluid pressure. The solid buffer curves were obtained by thermodynamic calculation under anhydrous conditions. As noted in Figures 6 and 8, the control points are rather sparse, and the values of f_{O_2} and in particular f_{S_2} capable of being fixed simultaneously are rather limited, due to the lack of suitable solid buffer assemblages.

Tungstenite appears to have a rather wide field of stability, which seems inconsistent with its very rare occurrence in nature. The absence of Mo competing with W for sulfur to form molybdenite may be partly responsible (*e.g.* Krauskopf, 1970). Also, in a system where Ca is available, tungstenite loses a wide log f_{O_2}–log f_{S_2} stability field to scheelite (Hsu, 1975). However, because of its similarity to molybdenite in physical properties and X-ray diffraction pattern, tungstenite may have been misidentified as molybdenite on many occasions in the field as well as in the laboratory, when its identity was not confirmed by chemical analysis. The equilibrium curve for reaction (6) passes through these points on the log f_{O_2}–log f_{S_2} diagram: (−19.4, −3.0), (−21.8, −7.1), and (−24.9, −12.7) at 577°C and 1000 bars.

No experimental data are available for conditions

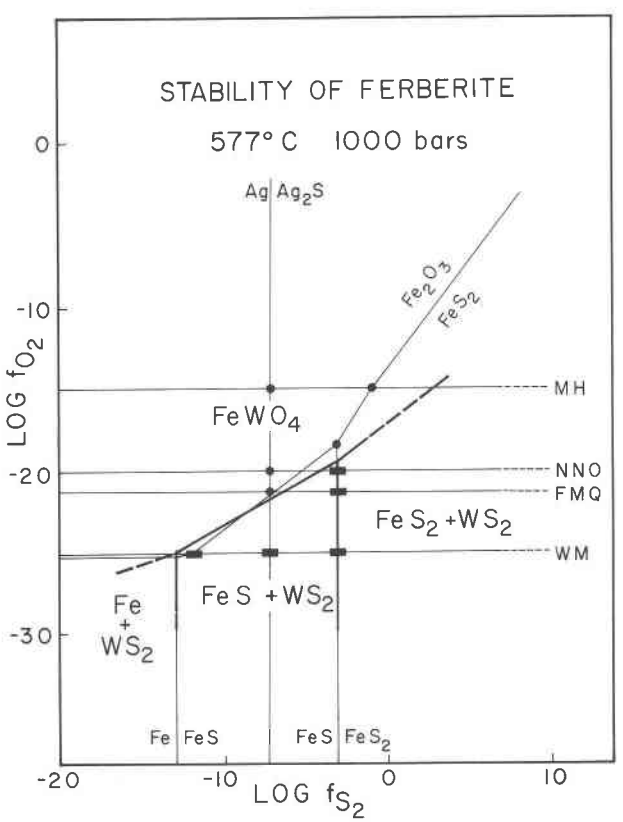

FIG. 6. The stability of ferberite as a function of f_{O_2} and f_{S_2} at T = 577°C and P_f = 1000 bars.

TABLE 3. Experimental results of wolframite stability as a function of f_{O_2} and f_{S_2} at T = 577°C and P_f = 1000 bars

Run No.*	Starting Mix	Buffer(s)	Duration (Hours)	Condensed Run Products**
FB 153	Tn+Po+Fb	MPH	329	Fb+(Tn+Py)
152	Tn+Po+Fb	MPR	810	Fb+(Tn+Po+Py)
150	Tn+Po+Fb	PR and NNO	552	Tn+Po+Py+(Fb)
142	Tn+Po+Fb	PR and FMQ	232	Tn+Po+Py+(Fb)
143	Tn+Po+Fb	PR and IW-WM	232	Tn+Po+Py
169	Tn+Po+Fb	SA and MH	477	Fb+(Tn+Po)
149	Tn+Po+Fb	SA and NNO	620	Fb+(Tn+Po)
170	Tn+Po+Fb	SA and FMQ	477	Fb+(Tn+Po)
148	Tn+Po+Fb	SA and IW-WM	600	Tn+Po
155	Tn+Po+Fb	IWR-WMR	281	Tn+Po
HB 22	Tn+Ad+Hb	MPH	555	Hb+(Tn+Ad)
21	Tn+Ad+Hb	MPR	1032	Hb+(Tn+Ad)
31	Tn+Ad+Hb	PR and NNO	546	Hb+(Tn+Ad)
36	Tn+Ad+Hb	PR and FMQ	613	Tn+Ad+(Hb)
24	Tn+Ad+Hb	SA and MH	575	Hb
28	Tn+Ad+Hb	SA and NNO	546	Hb+(Tn+Ad)
35	Tn+Ad+Hb	SA and FMQ	472	Hb+(Tn+Ad)
30	Tn+Ad+Hb	SA and IW-WM	472	Tn+Ad+(Hb)
34	Tn+Ad+Hb	IWR-WMP	472	Tn+Ad+(Hb)

* and ** Same as ** and *** in Table 2, respectively.

with f_{S_2} values above those defined by the $Fe_{1-x}S$–FeS_2 assemblage and below those defined by the Fe–$Fe_{1-x}S$ assemblage. The slopes of the boundary curves for ferberite and its sulfide counterparts in these regions are inferred from topological analysis, as shown in Figure 7. The figure also suggests that, in a system with excess Fe, ferberite can survive to conditions of much higher f_{O_2} and f_{S_2} where it coexists with pyrite.

The introduction of sulfur into the hydrothermal system of huebnerite bulk composition gives rise to the following reaction

$$MnWO_4 + 3/2\ S_2 = WS_2 + MnS + 2O_2 \qquad (7)$$

The result is similar to that for ferberite, except that tungstenite is accompanied by alabandite, MnS, instead of iron sulfides. Figure 9 indicates that huebnerite has a slightly wider stability field than ferberite at high f_{O_2} and f_{S_2} conditions.

The effects of confining pressure and temperature on the stability of ferberite and huebnerite in the log f_{O_2}–log f_{S_2} field were not determined. However, the effect of pressure on the stability field boundaries, particularly at high temperatures, can be safely ne-

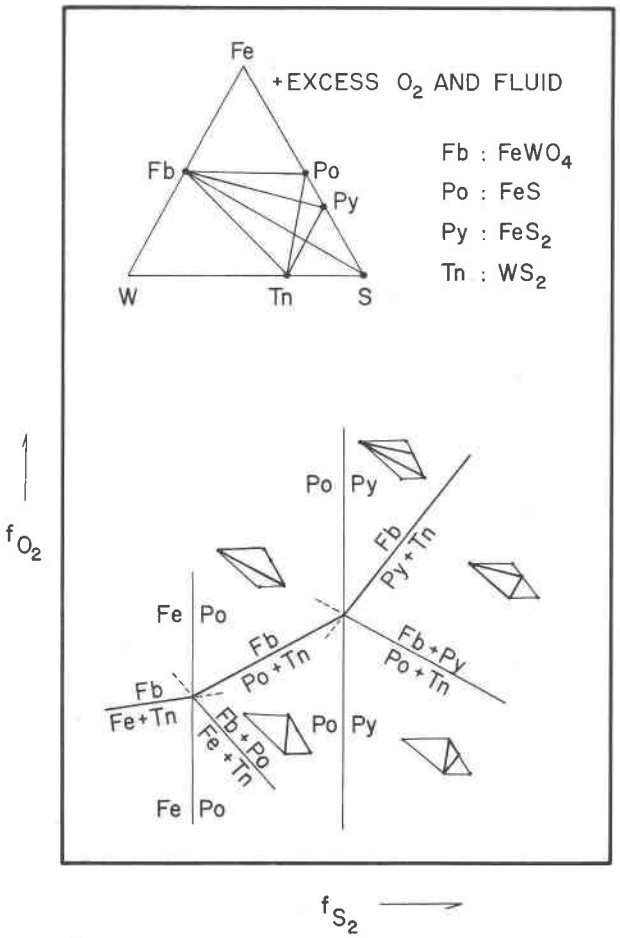

FIG. 7. The f_{O_2}–f_{S_2} relations of the phases in the system Fe–W–O–S.

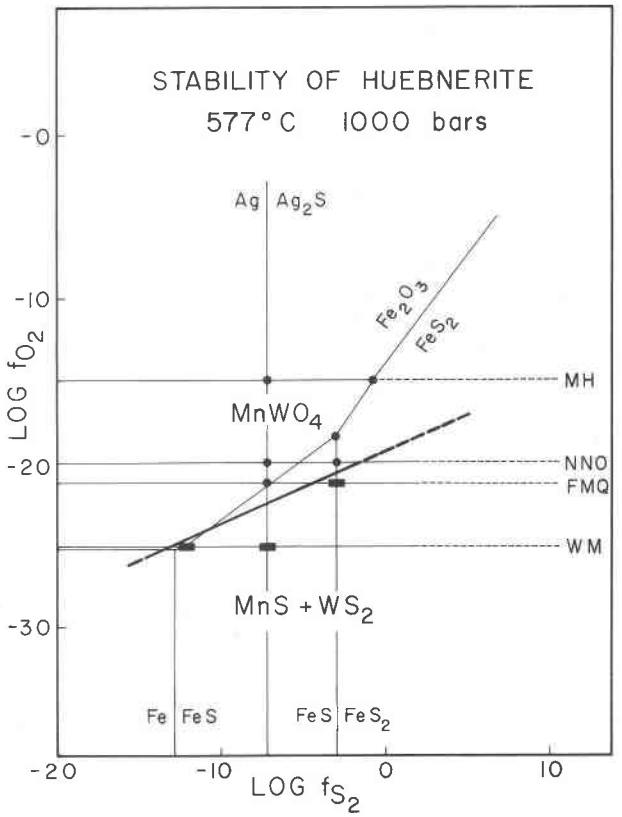

FIG. 8. The stability of huebnerite as a function of f_{O_2} and f_{S_2} at T = 577°C and P_f = 1000 bars.

glected in the pressure range of a few thousand bars, since the ΔV's of the reactions (6) and (7) are small, resulting in pressure corrections $\lesssim 0.08\ P-1/T$. Temperature changes of a few hundred degrees will undoubtedly shift the position of the equilibrium curves with respect to log f_{O_2} and log f_{S_2}, but the positions of the curves relative to those of the solid buffer assemblages probably are not greatly affected. At low temperatures, MnS_2 might be encountered, in addition to MnS, and would modify the equilibrium curves. Eugster and Skippen (1967) calculated the fugacities of the more abundant gas species in the system H–O–S internally controlled by the three buffer assemblages, pyrrhotite + iron + magnetite or wüstite, pyrrhotite + pyrite + magnetite, and hematite + pyrite + magnetite at 2000 bars pressure. As those gas species other than oxygen and sulfur do not participate in the reaction, their presence should not affect the equilibrium.

Conclusions

Although detailed data for intermediate members of the series are not available, some conclusions may be drawn based on the data obtained for the two end members. A complete solid solution series exists between ferberite and huebnerite over the experimental temperature range of 400° to 900°C and 1000 bars. Each intermediate member can be synthesized within this range with f_{O_2} buffered in the vicinity of NNO. Thus, contrary to some previous statements, temperature alone cannot be held responsible for compositional variation of natural wolframites crystallized under oxygen fugacities approximating those of the NNO buffer. This conclusion is supported by the work of Barabanov (1961), who found that the composition of wolframite varies considerably not only in a given deposit but in a single vein. The temperature of wolframite mineralization is best determined by using fluid inclusions rather than compositional variations, as is shown by Naumov and Ivanova (1971).

The unusually strong resistance to oxidation shown by ferberite nullifies the effect of f_{O_2} on the

composition of wolframite. Wolframite of any composition can remain stable under the oxidation states prevailing in hydrothermal environments. The stability fields of ferberite and huebnerite do not differ appreciably in the presence of both oxygen and sulfur. Apparently neither f_{O_2} nor f_{S_2} exerts any noticeable influence on the composition of wolframite. The wide stability field of tungstenite suggests that it may be more widespread in sulfur-rich environment than commonly thought, although the presence of molybdenum and calcium may inhibit its formation.

Variations in the Mn/Fe ratio of the source material probably is the most important factor in controlling wolframite composition, although the pH of the ore solution may have some influence, as suggested by experimental work on silicotungstic acid (Gundlach, 1967). Thus, the variation of the Mn/Fe ratio in wolframite is of little value as a clue to the important physico-chemical variables during ore formation, such as temperature, pressure, f_{O_2} and f_{S_2}. The temperature-independence, in particular, helps settle the controversy among many workers.

Acknowledgments

Critical reviews of the manuscript by G. Kullerud and G. Millholen of Purdue University, S. D. Scott of University of Toronto, J. S. Huebner of the U.S. Geological Survey, and J. H. Schilling of University of Nevada, Reno, are gratefully acknowledged. This investigation was supported by the National Science Foundation Grant GA 35322.

References

Appleman, D. E. and H. T. Evans, Jr. (1973). Indexing and least-squares refinement of powder diffraction data. *U. S. Natl. Tech. Inform. Serv.* **PB 216–188.**

Arnold, R. G. (1966). Mixtures of hexagonal and monoclinic pyrrhotite and the measurement of the metal content of pyrrhotite by X-ray diffraction. *Am Mineral.* **51,** 1221–1227.

Barabanov, V. F. (1961). *Mineralogy of East Transbaikalian Wolframite Deposits.* Vol. 1, Leningrad University Press.

Barnes, H. L. (1971). Investigations in hydrothermal sulfide systems. In, G. C. Ulmer, Ed., *Research Techniques for High Pressure and High Temperature.* Springer-Verlag, New York, p. 317–356.

Baumann, L. and R. Starke (1964). Beitrag zur Verteilung der H/F Koeffizienten innerhalb der Wolframitlagerstätte Pechtelgrün auf Grund neuer röntgenographischer Untersuchungen. *Bergakademie,* **16,** 79–82.

——— and ——— (1965). Genetic interpretation of wolframite deposits by means of X-ray analysis of wolframite. Symp.: *Problems of Postmagmatic Ore Deposits.* Vol. 11, Prague, 1963, 572–576.

Bayer, G. (1962). Isomorphie- und Morphotropiebeziehungen bei Oxyden mit TiO_2-typ und verwandten Strukturen. *Ber. Dtsch. Keram. Gesel.* **39,** 535–554.

Berman, J. and W. Campbell (1957). Relationship of composition to thermal stability in the huebnerite–ferberite series of tungstates. *U. S. Bur. Mines Rep. Invest.* **5300,** 14 p.

Boettcher, A. L. and D. M. Kerrick (1971). Temperature calibration in cold-seal pressure vessels. In, G. C. Ulmer, Ed., *Research Techniques for High Pressure and High Temperature.* Springer Verlag, New York, p. 179–194.

Bolduan, H. (1954). Genetische Untersuchung der Wolframitlagerstätte Pechtelsgrün (Vogtl.) unter besonderer Berücksichtigung der Verteilung des H/F Koeffizienten im Wolframit. *Freiberg Forsch.* **C10,** 46–62.

Churikov, V. S. (1959). Certain features of the chemical composition of wolframites. In, *Materials Relating to Geology, Petrography, Mineralogy, and Geochemistry of Ore Deposits.* Izd-vo An. SSSR, Moscow.

Escobar, C., H. Cid-Dresdner, P. Kittl and I. Duemler (1971). The relation between 'light wolframite' and common wolframite. *Am. Mineral.* **56,** 489–498.

Eugster, H. P. (1957). Heterogeneous reactions involving oxidation and reduction at high pressure and temperature. *J. Chem. Phys.* **26,** 1760–1761.

——— and G. B. Skippen (1967). Igneous and metamorphic reactions involving gas equilibria. In, P. H. Abelson, Ed., *Researches in Geochemistry.* Vol. 2, Wiley and Sons, Inc., New York, p. 492–520.

——— and D. R. Wones (1962). Stability relations of the ferruginous biotite, annite. *J. Petrol.* **3,** 82–125.

Ganeev, I. G. and N. P. Sechina (1960). Geochemical peculiarities of wolframite. *Geokhimiya,* 518–523. [transl. *Geochem.* 617–623 (1960)].

Gundlach, H. (1967). Transport und Abscheidungsbedingungen von Wolframerzen aus Wasserigenlösungen. In, *Pegmatische Lagerstätten und Ihre Wirtschaftliche Bedeutung,* H. 19, Clausthal-Zellerfeld.

Hsu, L. C. (1968). Selected phase relationships in the system Al–Mn–Fe–Si–O–H: a model for garnet equilibria. *J. Petrol.* **9,** 40–83.

——— (1975). Effects of oxygen and sulfur fugacities on the scheelite–tungstenite and powellite–molybdenite stability relations (abstr.). *Geol. Soc. Am. Abstr. Progr.* **7,** 1123.

Huebner, J. S. (1971). Buffering techniques for hydrostatic systems at elevated pressures. In, G. C. Ulmer, Ed., *Research Techniques for High Pressure and High Temperature,* Springer-Verlag, New York, p. 123–178.

——— and M. Sato (1970). The oxygen fugacity–temperature relationships of manganese oxide and nickel oxide buffers. *Am. Mineral.* **55,** 934–953.

Kittl, E. (1951). Sobre la wolframita liviana de Liquinaste, Jujuy. *Rev. Minera,* **20,** 56–61.

——— and P. Kittl (1965). Der leichte Wolframit von Liquinaste, Jujuy in Argentinien. *Aufschluss,* **16,** 52–54.

Krauskopf, K. B. (1957). The heavy metal content of magmatic vapor at 600°C. *Econ. Geol.* **52,** 786–807.

——— (1970). Tungsten (Wolfram). In, K. H. Wedepohl, Ed., *Handbook of Geochemistry II,* Springer-Verlag, Berlin.

Lawrence, L. J. (1961). Crystal habit of wolframite as an indication of relative temperature of formation. *Neues Jahrb. Miner. Monatsh.,* 241–247.

MacRae, N. D. and G. Kullerud (1972). Preliminary investigation of almandine–sulfur–water at 700°C, 1 Kb. *Can. Mineral.* **11,** 563–566.

Naumov, V. B. and R. F. Ivanova (1971). The pressure and temperature conditions for formation of wolframite deposits. *Geokhimiya,* **6,** 627–641. [transl. *Geochem. Int.* **8,** 381–394 (1971)].

Robie, R. A. and D. R. Waldbaum (1968). Thermodynamic

properties of minerals and related substances at 298.15°K (25.0°C) and one atmosphere (1.013 bars) pressure and at higher temperatures. *U. S. Geol. Surv. Bull.* **1259,** 1–255.

ROTH, R. S. AND J. L. WARING (1966). Phase equilibria as related to crystal structure in the system niobium pentoxide–tungsten trioxide. *J. Res. Natl. Bur. Stand.* **70A,** 281–303.

SASAKI, A. (1959). Variation of unit-cell parameters in wolframite series. *Mineral. J. (Japan)* **2,** 375–396.

SCHRÖCKE, H. (1969). Über Festkörpergleichgewichte in System Fe–Mn–W–O. *Neues Jahrb Mineral. Abh.* **110,** 115–127.

——— AND A. TRUMM (1968). Über die Bestimmung des thermodynamischen Parameter kristalliner oxydischer Mischphasen mittels Sauerstoffpartialdruckmessung. *Neues Jahrb. Miner. Abh.* **109,** 1–14.

SLEIGHT, A. W. (1972). Accurate cell dimensions for ABO_4 molybdates and tungstates. *Acta Crystallogr.* **B28,** 2899–2902.

TANISAKI, S. (1960a). The phase transition of tungsten trioxide below room temperature. *J. Phys. Soc. Japan,* **15,** 566–573.

——— (1960b). Crystal structure of monoclinic tungsten trioxide at room temperature. *J. Phys. Soc. Japan,* **15,** 573–581.

TAYLOR, R. G. AND K. F. G. HOSKING (1970). Manganese–iron ratios in wolframite, South Crofty mine, Cornwall. *Econ. Geol.* **65,** 47–53.

TRUNOV, V. K. AND L. M. KOVBA (1966). Interaction of molybdenum and tungsten trioxides with iron and chromium sesquioxides. *Izv. Akad. Nauk. SSSR, Neorg. Materialy,* **2,** 151–154. [transl. *Inorg. Mater.* **2,** 127–130 (1966)].

TUTTLE, O. F. (1949). Two pressure vessels for silicate–water studies, *Geol. Soc. Am. Bull.* **60,** 1727–1729.

UEDA, R. AND T. ICHINOKAWA (1951). On the phase transition of tungsten trioxide. *Phys. Rev.* **82,** 563–664.

Manuscript received, September 26, 1975; accepted for publication, February 25, 1976.